Journal of Thermal Analysis and Calorimetry, Vol. 82 (2005) 137–142

STUDY OF SOME PHENOLIC–IODINE REDOX POLYMERIC PRODUCTS BY THERMAL ANALYSES AND MASS SPECTROMETRY

M. A. Fahmey[1], *M. A. Zayed*[2*] *and H. G. El-Shobaky*[2]

[1]Nuclear Physics Department, N.R.C., Atomic Energy Authority, Cairo 13759, Egypt
[2]Chemistry Department, Faculty of Science, Cairo University, Giza, Egypt

This paper describes the use of the mass spectrometry (MS), thermal analyses (TA) and other physico-chemical methods to investigate the structure of two newly synthesized phenolic-iodine derivative polymeric products. These two products are formed as a result of redox-interaction of adrenaline hydrogen tartrate (AHT, **I**) with iodate (IO_3^-) and periodate (IO_4^-). The characterization of the two products were achieved satisfactorily by using the above tools and their proposed general formulae, were found to be $C_{52}H_{67}O_{36}N_4I$ (AHT–IO_3^-, **II**) and $C_{26}H_{34}O_{18}N_2I_2$ (AHT–IO_4^-, **III**).

The fragmentation behavior of the main compound (AHT) in MS and TA (TG and DTA) techniques was investigated and compared. The results obtained were used to explain the fragmentation of the products AHT–IO_3^- and AHT–IO_4^- in mass spectrometry and thermal analyses techniques. The stabilities of different fragments were discussed.

The results indicate that the two techniques are supporting each other in which the mass spectrometry provides the structural information in gas phase while the thermal analyses provides the quantitative fragmentation in the solid-state.

Keywords: *mass spectrometry, redox reactions, thermal analysis*

Introduction

Polyphenols are widely distributed in nature. They occur in most plants and are components of many beverages manufactured from plant sources [1]. Catecholamine is a common constituent of many biological systems, which have variety of roles in these systems [2–5].

The structure of phenols and their redox products were generally based upon information obtained by using different mass spectrometric techniques [6–10]. Special advantages in structural studies were obtained from combination between mass spectrometry, infra-red spectroscopy and thermogravimetry [11]. Investigation of some phenolic compounds using mass spectrometry in comparison with thermal analyses was performed by Zayed *et al*. [12, 13]. This is very important in order to identify the chemical processes and the fragmentation. The EI and TA fragmentation do not necessary follow the same pathways. The success of comparison between two techniques, in structure confirmations is based on the correct choice of the unimolecular fragmentation channel of decay in MS and TA [12].

The aim of the present work is the use of the mass spectral fragmentation in comparison with thermal decomposition of compounds **I**–**III** and other physico-chemical methods chiefly to confirm and to elucidate the general and structural formulae of the two products **II** and **III**.

Experimental

Synthesis of AHT–IO_3^- (II) and AHT-IO_4^- (III)

AHT–IO_3^- was prepared by adding 100 mL of 0.1 M IO_3^- to 100 mL 0.1 M AHT at 70°C and pH 4–5. The formed precipitate was left in contact with the mother liquor for 2 h. The precipitate was filtered and washed with hot distilled water several times and finally with pure ethanol then dried in air. While AHT–IO_4^- product was prepared by dissolving 1.666 g of AHT in 100 mL of water and then added to 100 mL of 0.025 M IO_4^- at 20°C and pH 5–6. The formed redox products were recrystallized from ethanol and their m.p.s were measured.

Instrumentation

Microanalyses of the products **II** and **III**

Microanalyses of C, H and N and molecular mass determinations of the pure products were performed at the Microanalytical Center of Cairo University.

Infrared spectroscopy

The IR spectra of the solid products were recorded using KBr disc technique in the wave number range 250–4000 cm^{-1}, using Perkin-Elmer model 1650 FTIR.

* Author for correspondence: mazayed429@hotmail.com

1388–6150/$20.00

Akadémiai Kiadó, Budapest, Hungary
Springer, Dordrecht, The Netherlands

Mass spectral measurements

The electron impact (EI) ionization of the studied compounds was conducted on a Hewlett-Packard (Palo Alto, CA, USA) mass spectrometer, model 5988 at the microanalytical Center, Cairo University. 70 eV was selected as the ionization energy and samples were introduced by the direct-insertion probe (DIP) technique. The ion source temperature was maintained at 200°C and the DIP was initially heated to 50°C and its temperature was then gradually raised to 200°C. The trap current was adjusted to 10 μA and the electron multiplier maintained at 1500 V. The instrument was calibrated by using perfluorotributylamine as standard.

Thermal analyses (DTA and TG)

DTA and TG studies were made with conventional thermal analyzer (Shimadzu system and 30 series thermal analyses instrument DTA-50H and TG-50H). The mass losses (of 5 mg sample) and heat response of the changes in the sample were measured from the ambient temperature to 600°C with heating rate 10°C min^{-1} in both TG and DTA in an inert argon atmosphere. These instruments were calibrated using indium metal as a thermally stable material. The reproducibility of the instrument reading was determined by repeating each experiment twice.

Results and discussion

The main compound AHT (**I**) together with its iodine redox solid products (AHT–IO_3^-, **II** and AHT–IO_4^-, **III**) were studied by means of mass spectrometry in comparison with thermal analyses and other physico-chemical methods as elemental analysis and IR spectroscopy, aiming to identify their actual structures.

*Microanalysis and IR characteristics of the products **II** and **III***

The results of elemental analyses of the two compounds (**II**–**III**) together with some of their properties as well as their general formulae are shown in Table 1. The IR spectral bands assignment of the products **II** and **III** is given in Table 2.

The proposed structures of the produced compounds **II**–**III**, as gained from the results of the microanalyses and infrared spectroscopy with well-known compound **I** are given.

*Thermal analyses (TG and DTA) of the products **I**–**III***

TG curve (Fig. 1a) of AHT (**I**) exhibits four stages (Scheme 1) of mass losses at temperature ranges; 25–190, 190–250, 250–330 and 330–400°C. These stages involved mass losses of 13.3, 31.3, 8.7 and 13.3%, respectively (the calculated total mass losses= 66.2 %). These mass losses (Table 3) may be due to successive loss of CO_2, $C_3H_6O_4$, CH_3NH and $CH(OH)–CH_2$ at the given temperature ranges respectively. DTA curve (Fig. 1a) displays four endothermic peaks. The first one is strong and centered at 158°C. The second peak is broad with its maximum at 196°C. The third and fourth peaks are weak and occur at 260 and 340°C, respectively (Scheme 1).

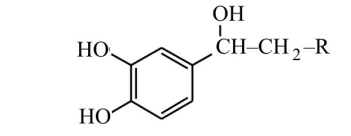

R=$CH_3NH–HCOO(CH–OH)_2COOH$

Mol mass=333

AHT (**I**)

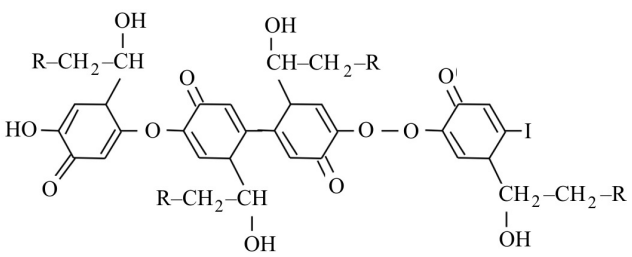

Mol mass=1451

AHT–IO_3^- (**II**)

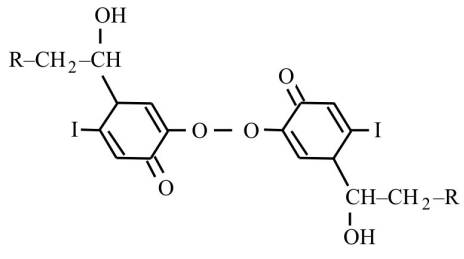

Mol mass=916

AHT–IO_4^- (**III**)

Compounds I–III

Table 1 Microanalysis of solid products **II** and **III**

Redox products	*m. p.*/°C	Colour	C/%		H/%		N/%		Molecular mass		General molecular formula
			calc.	found	calc.	found	calc.	found	calc.	found	
II AHT–IO_3^-	>300	black	43.5	43	4.9	4.6	3.9	3.9	1451	1450	$C_{52}H_{67}O_{36}N_4I$
III AHT–IO_4^-	>300	black	31.5	31.1	3.6	3.7	3.2	3.1	916	916–950	$C_{26}H_{34}O_{18}N_2I_2$

Table 2 The FTIR spectra of the solid products **II** and **III**

Compound	Band ν / cm^{-1}	Intensity/%	Assignment
II AHT–IO_3^-	3114–3431	40–46	Due to ν_{OH} of different OH groups in aromatic system and aliphatic side chains.
	1720	34	Due to the $\nu_{=O}$ of carbonyl groups in the conjugate semi-quinone system.
	1601	6	Due to V_{C-O} of the peroxide and other bonds.
	1215–1446	30	Due to carboxylic groups in side chains of tartrate groups.
	576–1077	50–72	Due to the different modes of the ring systems.
	490, 44	72–75	May be due to the modes of the two symmetrical C–I groups.
III AHT–IO_4^-	3232–3747	39–90	Due to the ν_{OH} of OH groups of temperature of IV dimer or the OH of side chain together with ν_{OH}.
	1608	6	Due to ν_{C-O} of peroxide dimer.
	1241–1453	25–29	Due to different modes of aliphatic chain.
	670–1079	74–51	Due to the different modes of the ring system of the bulky dimer.
	419	87	Due to the modes of the identical C–I of iodine in symmetrical dimer.

TG curve (Fig. 1b) of the reaction product AHT – IO_3^- (**II**) is composed of four stages (Scheme 2) at temperature ranges; 25–125, 125–275, 275–560 and 560–600°C. These stages correspond to the mass losses of 8.5, 5.2, 72.8 and 3.8%, respectively. The DTA curve (Fig. 1b) consists four endothermic peaks. These peaks are broad and weak except the second one, which is sharp. The maxima of these peaks are initiated by that located at 59 (due to H_2O and $C_3H_6O_4$ loss) followed by peaks at 264, 299 and 589°C, respectively (Scheme 2).

TG curve (Fig. 1c) of the redox product AHT – IO_4^- (**III**) consists of two stages (Scheme 3) ranged between 25–315 and 315–580°C. They are accompanied by mass losses of 30 and 61%, respectively. DTA curve (Fig. 1c) comprises of four endothermic peaks initiated by that located at 56°C (may be due to loss of H_2O, $C_3H_6O_4$ and CO_2 loss) followed by peaks at 300, 471 and 591°C (Scheme 3).

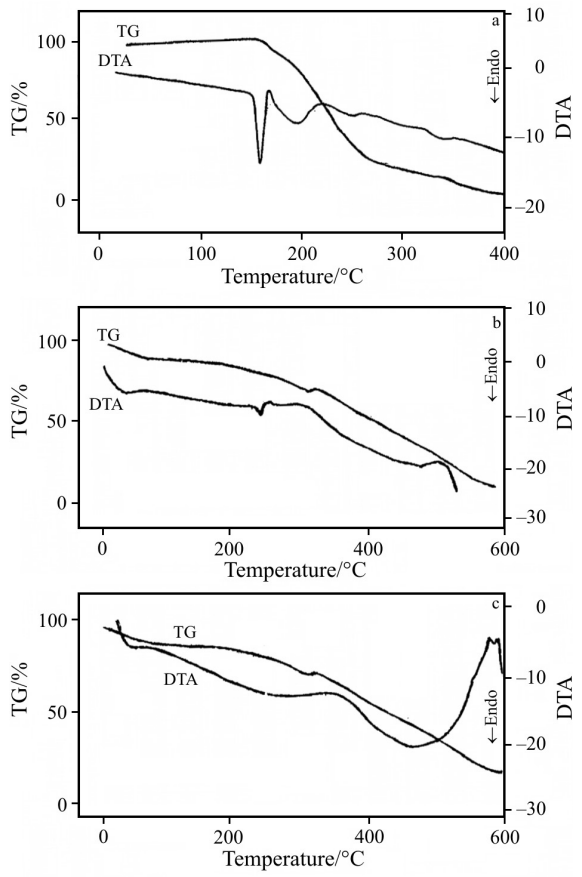

Fig. 1 TG and DTA curves of the main compound a – AHT and the products b – AHT–IO_3^- and c – AHT–IO_4^-

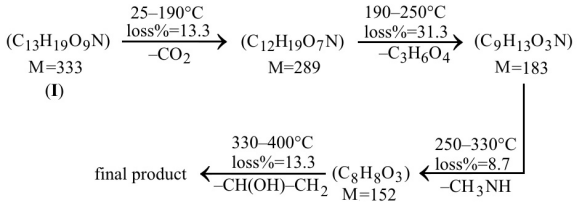

Scheme 1 Thermal decomposition behavior of AHT

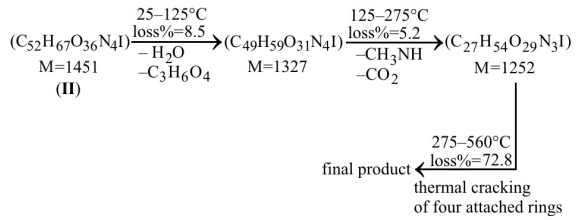

Scheme 2 Thermal decomposition behavior of AHT–IO_3^- product

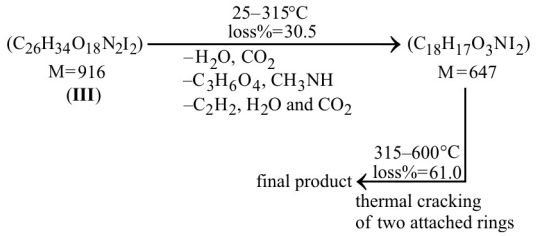

Scheme 3 Thermal decomposition behavior of AHT–IO_4^- products

*Mass characteristics of the compounds **I–III***

The electron impact mass spectra of the main compound (AHT) and its redox products (AHT–IO_3^- and AHT–IO_4^-) were recorded and investigated at 70 eV of electron energy. The important peaks and their relative abundance for the molecular ion up to *m*/*z* 55 (only prominent and important peaks are recorded for simplification) are listed in Table 4. The main fragmentation pathway following electron impact of AHT is due to successive loss of CO_2+H_2O followed by $C_3H_6O_4$ loss (Scheme 4) forming fragment ions at *m*/*z*=271 and 165 (Table 4). Fragment ion at *m*/*z*=165 (R.A.=100%, base peak) which is the dehydrated adrenaline, can undergo CH_2NH and C_2H_2 loss [14] to form dihydroxybenzene (Scheme 4). The H_2O loss take place from hydroxyl groups located on alkyl side chain but not from two hydroxyl groups of the phenyl rings [14].

The mass spectrum of the product AHT–IO_3^- (**II**) is characterized by low relative abundance of higher masses (Table 4) which may be due to low stability of the fragment included four attached rings. The appearance of signals at masses *m*/*z*=1055, 857 and 629 is mainly due to successive loss of 2(R+H_2O) (one step) and 2(R+H_2O) stepwise (Scheme 5). The mass spectrum of the product AHT–IO_4^- (**III**) is characterized by two intense peaks at *m*/*z*=352 (R.A.=100%, base peak) and at *m*/*z*=426 (R.A.=80%, second prominent peak). These fragment ions are reasonably due to the cleavage at bridging bond between O–O, followed by competitive loss of $C_3H_6O_4$ and CH_3OH from molecular ion (i.e $C_{10}H_{11}O_4NI$ and $C_{12}H_{13}O_7NI$). Another possible pathway (Scheme 6) is due to successive loss 2(R+H_2O) stepwise followed by $2C_2H_2$ loss followed by $2CH_3I$ loss stepwise (appearance ions at 718, 520, 466, 324, 182) (Scheme 6). The latter pathway is selected for comparison.

The mass spectra of the three compounds **I**–**III** demonstrate the molecular ions peak of *m*/*z* 333, 1451 and 916 for **I**–**III**, respectively, with a very low relative abundance (< 1%) at 70 eV. The abundance of the molecular ion depends mainly on the structure and therefore the potential energy surface of the molecular ion [15]. On the other hand, in EI ionization the molecular ion peak may have low abundance and often many fragments are observed [15]. Also, the com-

Table 3 Thermal analyses of the main compound (AHT) and the products AHT–$IO_3^-$and AHT–IO_4^-

Compound	T_{range}/°C	Mass loss/%		Possible fragments	DTA
		calc.[a]	est.[b]		
I AHT	25–400	66.5	66.7	CO_2, $C_3H_6O_4$, CH_3NH, $CH(OH)–CH_2$	At 158°C: end peak, loss of CO_2. At 196°C: end peak, loss of $C_3H_6O_4$. At 260°C: end peak, loss of CH_3NH. At 340°C: end peak, loss of CH_3CHO.
II AHT–IO_3^-	25–600	90.3	91.2	H_2O, $C_3H_6O_4$, CO_2 CH_3NH and thermal cracking of 72% of the total mass including rupture of four attached rings.	At 59°C: end peak, loss of H_2O, $C_3H_6O_4$. At 284°C: end peak, loss of CH_3NH_2, CO_2. At 299°C and at 589°C end peaks (undefined fragments).
III AHT–IO_4^-	25–600	92.5	93	H_2O, CO_2, $C_3H_6O_4$, CH_3NH, C_2H_2, H_2O and CO_2 , and thermal cracking of 61% of the total mass including rupture of two attached rings.	At 56°C: end peak, loss of H_2O, CO_2. At 300°C: end peak, loss of R, ethanol. At 471°C: end peak, loss of $2CH_3I$. At 471 and 591°C end peaks (undefined fragments).

[a]Calculated mass loss from the mol of the compound, [b]Estimated percent loss from experimental work

Table 4 Relative abundances (%) of principal fragments in the mass spectra of the compounds **I**–**III**

Compound	*m*/*z* (R.I.)									
AHT	333 (<1)	271 (47.5)	165 (100)	136 (77.8)	110 (68.8)	81 (66.2)	55 (98.0)			
AHT– IO_3^-	1451 (<1)	1055 (2.3)	857 (1.8)	659 (2.4)	415 (1.53)	386 (2.9)	218 (11.4)	156 (39.8)	83 (67.2)	55 (100)
AHT– IO_4^-	916 (<1)	718 (10.4)	520 (4.7)	466 (9.8)	426 (80.0)	353 (100)	324 (15.1)	182 (14.2)	81 (3.1)	55 (2.6)

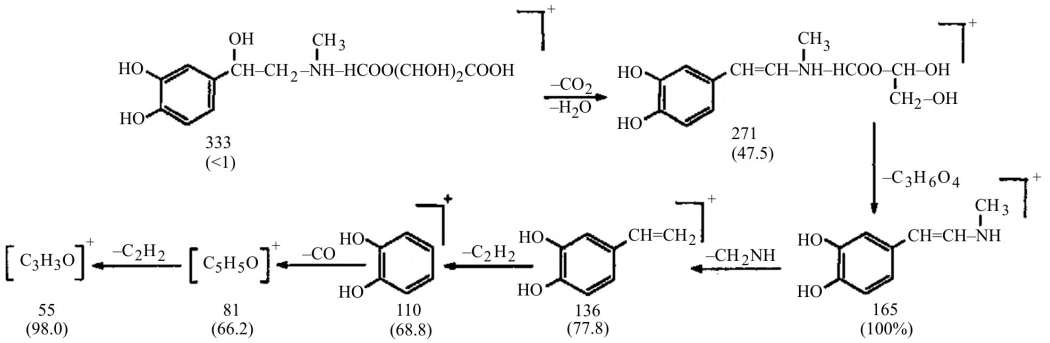

Scheme 4 MS fragmentation pathway of AHT

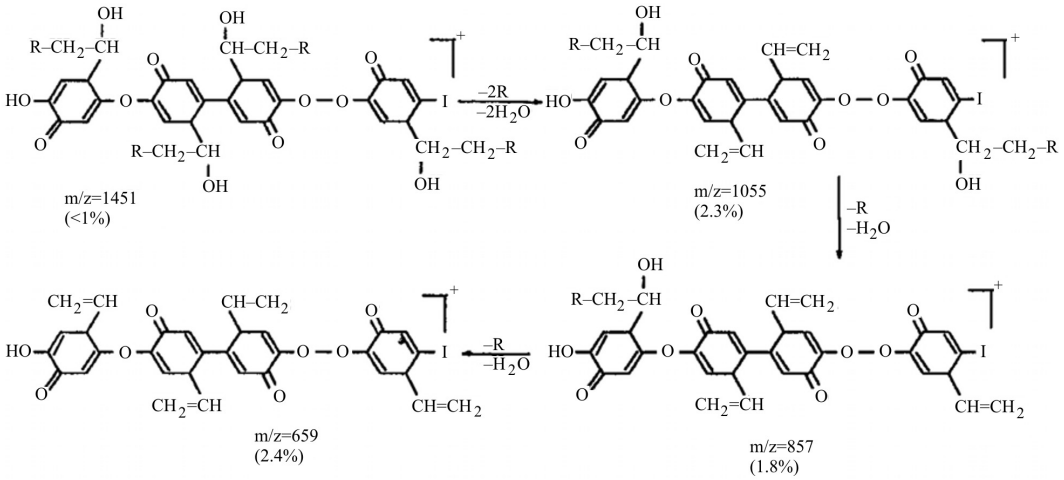

Scheme 5 MS fragmentation pathway of AHT–IO_3^- product

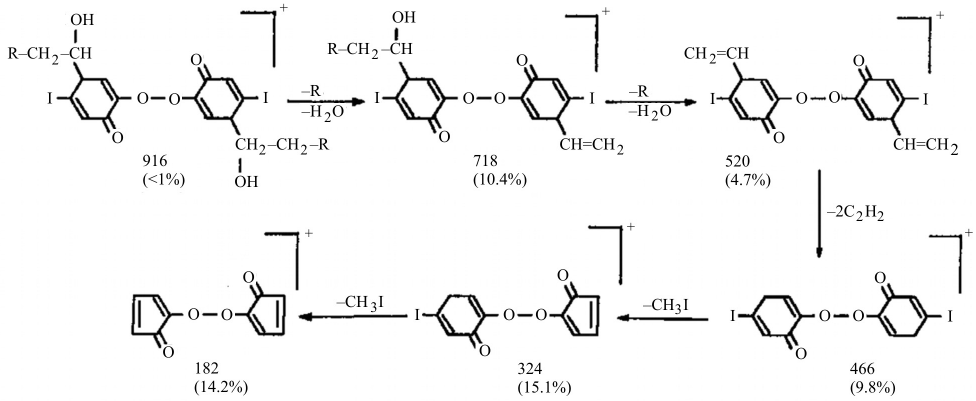

Scheme 6 MS fragmentation pathway of AHT–IO_4^- product

pounds **I** and **II** are characterized by very highly prominent abundant (≈98 %) at fragment ion *m*/*z*=55, while the product **III** has very low abundant (2.6%) at this fragment ion. This fragment ion is reasonably formed from $[C_5H_7O]^+$ (*m*/*z*=83) and $[C_5H_5O]^+$ (*m*/*z*=81) by CO and C_2H_2 loss, respectively. The proposed one channel fragmentation pathways for compounds **I–III**, are displayed in Schemes 4–6.

Comparative study between the behavior of fragmentation in TA and MS

In our previous study [12] the fragmentation of 2-hydroxyphenol (PC) and 2,3-dihydroxyphenol (PG) were investigated in both MS and TA techniques. Also, the three compounds formed as a result of reaction of these simple phenolic compounds (PC and PG) with IO_3^- and IO_4^- were investigated [13]. The comparative study be-

tween the behavior of fragmentation in TA and MS can be achieved by the careful inspection of Schemes 1–6 in comparison with each other. As example the case of compound **I**. The initial decomposition process of the compound AHT (**I**) is due to CO_2 loss from parent molecule (Scheme 1). In MS, additional to CO_2 loss as in TA, dehydration (i.e H_2O loss) occurs from the molecular ion forming a fragment ion at m/z=271 $[C_{12}H_{17}O_6N]^+$ in the mass spectra (Scheme 4 and Table 4). The initial compound is stable in TA up to 158°C (at range 25–190°C), while the molecular ion is unstable in MS (R.A. of $[M]^{+\cdot}$<1%). The rest mass (after CO_2 loss) has moderate stability in TA [decompose in range 190–250°C before subsequent $C_3H_6O_4$ loss (Scheme 1)]. In MS, the fragment ion $[M–CO–H_2O]^+$ (m/z=271) follows the same behavior as in TA (i.e. $C_3H_6O_4$ loss) and forms the most stable dehydrated adrenaline ($[C_9H_{11}O_2N]^+$, R.A.=100%). Subsequent decomposition in TA involves CH_3NH loss within the temperature range 250–300°C (direct bond cleavage), while in MS the fragment loss is CH_2NH [14] due to bond cleavage and H-rearrangement forming ion at m/z=136 (R.A.=77.8) (Scheme 4). At higher temperature range (330–400°C), the remainder losses CH(OH)–CH_2 fragment (cleavage the C–C bond between the ring and alkyl side chain, containing OH group), while in MS, the rupture of this C–C bond involves C_2H_2 loss and forming dihydroxyphenol ion ($[C_6H_6O_2]^+$, R.A.=68.8%). From this comparison it is concluded that, the initial products AHT–IO_3^- (four attached rings) and AHT–IO_4^- (two attached rings) are unstable in MS (ionized molecular ion in gas phase state), while in TA the two products are stable before initial decomposition to approximately the same temperature (59 and 56°C). Fragmentation of AHT–IO_3^- includes successive lose of fragments H_2O, $C_3H_6O_4$, CH_3NH, CO_2 before cleavage of the bonds between the four rings and mass loss of 72.8% from its original mass. On the other hand, addition fragments are lost from AHT–IO_4^- before thermal cracking of the bonds between the two attached rings within temperature range 315–600°C (mass loss=61%), in comparison to that of AHT–IO_3^- at 275–600°C. In MS the fragmentation of AHT–IO_3^- includes successive losses of 2R+2H_2O followed by R+H_2O twice before cleavage of the bonds between the rings. The product AHT – IO_4^- also initiated successive losses of R+H_2O followed by R+H_2O loss and additional fragmentation (Scheme 6) before complete decomposition of the product. Cleavage at the N–C bond (R loss) forming low stability fragment can be interpreted on the basis of the charge localization concept [16]. The non-bonding orbital available on the nitrogen atom is surely the site of electron expulsion upon ionization. The unpaired electrons have strong tendency to form a new bond, hence, the partial localization of unpaired electron in certain orbital can reduce the activation energy for cleavage of certain bonds.

Conclusions

Mass spectral fragmentation (MS), thermal analyses (TA) as well as IR spectroscopy and elemental analyses are utilized to study the two compounds obtained from the redox processes (AHT–IO_3^- and AHT– IO_4^-). Structure elucidation of these compounds was achieved satisfactorily. Also, the behavior of the main compound (AHT) is investigated using TA and MS. Comparative study of the fragmentation by MS and decomposition by TA was discussed and the data obtained were used to illustrate the behavior of the two redox products in both techniques. These techniques actually supported each other in elucidation of the structure of the two compounds.

References

1 J. P. Bartly, N. Whittle and G. Organ, in 'Advances in Mass Spectrometry' E. Gelpi, Ed., John Wiley & Sons, Chichester, 15 (2001) 813.
2 H. B. Niznik, Dopamine Receptors and Transporters. Pharmacology, structure and function, Marcel Dekker, New York 1994, p. 677.
3 S. E. Anderson, M. G. Peter and P. Roepstorff, Comp. Biochem. Physiol., 113B (1996) 689.
4 M. Sugumaran, Adv. Insect Physiol., 21 (1988) 179.
5 N. G. Lewis and L. B. Davin, in Isopentenoids and other Natural Products – Evolution and Function (W. D. Nesed), American Chemical Society, Washington D.C. 1994, p. 202.
6 M. Mann and M. Wilm, Trends Biochem. Sci., 20 (1995) 219.
7 P. Wheelan, J. A. Zirrolli and R. C. Murphy, J. Am. Soc. Mass Spectrom., 7 (1996) 140.
8 P. Schneider and M. A. J. Ferguson, Meth. Enzymol, 250 (1995) 614.
9 V. N. Reinhold, B. R. Reinhold and C. E. Costello, Anal. Chem., 67 (1995) 1772.
10 J. K. Kerwin, J. Mass Spectrom., 31 (1996) 1429; Rapid Comm. Mass Spectrom., 11 (1997) 557.
11 E. Kaisersberger and E. Post, Proc. Conf. North. Am. Therm. Anal. Soc., 26 (1998) 548.
12 M. A. Fahmey, M. A. Zayed and Y. H. Keshk, Thermochim. Acta, 366 (2001) 183.
13 M. A. Fahmey and M. A. Zayed, J. Therm. Anal. Cal., 67 (2002) 163.
14 H. -Y. Wu and Y.-P. Lin, Eur. J. Mass Spectrom., 6 (2000) 65.
15 F. W. McLafferty, Interpretation of mass spectrometry, Beniamin, London 1973.
16 K. Levsen, 'Fundamental Aspect of Organic Mass Spectrometry' Verlag Chemie Weinheim, New York 1978, p. 25.

Received: June 2, 2004

DOI: 10.1007/s10973-005-6454-9